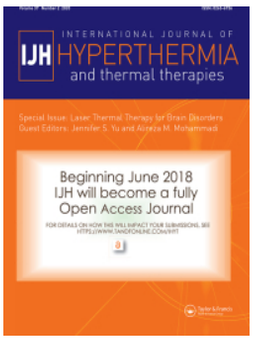

International Journal of Hyperthermia

ISSN: (Print) (Online) Journal homepage: https://www.tandfonline.com/loi/ihyt20

Non-thermal membrane effects of electromagnetic fields and therapeutic applications in oncology

Peter Wust, Ulrike Stein & Pirus Ghadjar

To cite this article: Peter Wust, Ulrike Stein & Pirus Ghadjar (2021) Non-thermal membrane effects of electromagnetic fields and therapeutic applications in oncology, International Journal of Hyperthermia, 38:1, 715-731, DOI: 10.1080/02656736.2021.1914354

To link to this article: https://doi.org/10.1080/02656736.2021.1914354

Published online: 28 Apr 2021.

INTERNATIONAL JOURNAL OF HYPERTHERMIA
2021, VOL. 38, NO. 1, 715–731
https://doi.org/10.1080/02656736.2021.1914354

Non-thermal membrane effects of electromagnetic fields and therapeutic applications in oncology

Peter Wust[a], Ulrike Stein[b] and Pirus Ghadjar[a]

[a]Department of Radiation Oncology, Charité – Universitätsmedizin Berlin, Corporate Member of Freie Universität Berlin and Humboldt-Universität zu Berlin, Berlin, Germany; [b]Experimental and Clinical Research Center, Charité – Universitätsmedizin Berlin and Max-Delbrück-Centrum (MDC), Berlin, Germany

ABSTRACT

The temperature-independent effects of electromagnetic fields (EMF) have been controversial for decades. Here, we critically analyze the available literature on non-thermal effects of radiofrequency (RF) and microwave EMF. We present a literature review of preclinical and clinical data on non-thermal antiproliferative effects of various EMF applications, including conventional RF hyperthermia (HT, cRF-HT). Further, we suggest and evaluate plausible biophysical and electrophysiological models to decipher non-thermal antiproliferative membrane effects. Available preclinical and clinical data provide sufficient evidence for the existence of non-thermal antiproliferative effects of exposure to cRF-HT, and in particular, amplitude modulated (AM)-RF-HT. In our model, transmembrane ion channels function like RF rectifiers and low-pass filters. cRF-HT induces ion fluxes and AM-RF-HT additionally promotes membrane vibrations at specific resonance frequencies, which explains the non-thermal antiproliferative membrane effects *via* ion disequilibrium (especially of Ca^{2+}) and/or resonances causing membrane depolarization, the opening of certain (especially Ca^{2+}) channels, or even hole formation. AM-RF-HT may be tumor-specific owing to cancer-specific ion channels and because, with increasing malignancy, membrane elasticity parameters may differ from that in normal tissues. Published literature suggests that non-thermal antiproliferative effects of cRF-HT are likely to exist and could present a high potential to improve future treatments in oncology.

ARTICLE HISTORY
Received 17 January 2021
Revised 31 March 2021
Accepted 1 April 2021

KEYWORDS
Non-thermal effects; electromagnetic fields; radiofrequency; amplitude modulation; hyperthermia

1. Introduction

Conventional radiofrequency (RF) hyperthermia (HT, cRF-HT) or microwave (MW) HT has been evaluated in clinical studies [1] and is used in the treatment of soft tissue sarcoma in combination with neoadjuvant chemotherapy [2], and for the treatment of cervical cancer [3–5] and superficial tumors [6–9], when combined with radiation therapy (RT). Annular phased array (APA) systems, capacitive systems (CS), and local RF or MW applicators are common technologies to achieve a specific absorption rate (SAR) of 10–60 W/kg in the target region and intended temperatures of $\geq$42 °C [10,11]. Current knowledge about cRF/MW-HT is based on numerous preclinical *in vitro* and *in vivo* studies mainly using water bath (WB) HT [12–17]. Generally, WB-HT kills tumor cells at temperatures $\geq$43 °C, but a combination of WB-HT with RT and/or chemotherapy might show efficacy at lower temperatures. Overgaard [14] described a relevant sensitization at 41.5 °C [thermal enhancement ratio (TER) of 1.34] if RT and HT are simultaneously applied. For sequential treatments however, nearly no cytotoxic effect was observed for temperatures $\leq$41 °C [17]. Thus, preclinical studies predict that temperatures above 41 °C are required for cRF/MW-HT to enhance the RT effects.

However, these requirements have not been usually achieved in all parts of the target for patients with deep-seated tumors (e.g., cervical cancer) in successful randomized studies investigating cRF-HT [4,5,18–21]. A conspicuous inconsistency between preclinical and clinical data remains as clinical trials using cRF-HT have demonstrated positive results. Improved reoxygenation and higher heat sensitivity of hypoxic (radioresistant) cells have been used to explain the favorable clinical results. Likewise, extreme whole body HT [22], a non-RF-based clinical counterpart of water bath HT, has resulted in disappointing clinical results even though the basic requirements, i.e., covering the target at temperatures >41.5 °C are always fulfilled.

Recently, a couple of clinical studies provided evidences of non-thermal effects in human tumors using AM-RF or RF. The researchers applied clinical systems like mEHT (modulated electro-hyperthermia [23,24], TTF (tumor treating fields) [25] and the TheraBionic device [26,27]. These studies have in common according to the general understanding of hyperthermia that temperature increases are below 40 °C and the observed effects are to be regarded as non-thermal.

CONTACT Peter Wust peter.wust@charite.de Department of Radiation Oncology, Charité – Universitätsmedizin Berlin, Corporate Member of Freie Universität Berlin and Humboldt-Universität zu Berlin, Berlin, Germany

Therefore, we hypothesize that additional non-thermal effects of the electromagnetic fields (EMF) exist and are clinically validated. This hypothesis is controversial as it challenges current textbook knowledge and has a high potential to impact clinical practice. Thus, we summarize the current information regarding the non-thermal effects of EMF.

2. Methods

We found an unmanageable number of hits in Google Scholar when we were searching for non-thermal biological effects of electromagnetic fields, such as 25,900 hits for the search term "non-thermal biological effects of electromagnetic fields" or even 1,900,000 hits for "electromagnetic field effects on cells". For the hyperthermia community, we assessed three clinical approaches (mEHT, TheraBionic and TTF) of maximum interest. Current studies with these approaches have been carefully analyzed to determine whether they provide evidence of non-thermal effects (Section 3). They were considered if they were either randomized or they used the EMF application alone. Hence, we discarded clinical phase I/II studies if EMF was used in combination with any other potentially effective schedule, as such studies might have a strong selection bias, making the clinical outcomes non-evaluable.

Then we took into account all publications that provided preclinical and methodological information for these clinical approaches. That is a considerable but manageable amount of work (Section 4).

In both sections, for clinical and preclinical studies the thermometry is crucial to differentiate between thermal and non-thermal effects. We evaluated not only the accuracy of the temperature measurements in selected points but also analyzed the setup in order to estimate the spatial temperature distribution. In particular, we had to discuss (and to exclude) unrecognized hot spots that are most frequently brought up in the field in order to refute non-thermal effects. If temperature measurements were missing, we attempted a reliable estimation of the temperature from the applied power and resulting SAR (specific absorption rate) distribution.

It is a frequent objection to the existence of non-thermal effects that no convincing physical explanations have been found so far. Thus, the presentation of biophysical and electrophysiological models, which are able to explain such effects, is a central part of this work (Section 5). We emphasize that such a theoretical framework is novel but is deduced from a still incomplete database. Verification or even establishment of a final theory about membrane effects of EMF was neither intended nor possible.

3. Clinical studies

Regional cRF-HT can reach intermediate temperatures of 39–43 °C in larger areas and is suitable for extended cancer diseases. Typically, total powers of >500 W are applied using the most advanced APA systems. The gained temperatures are nevertheless not sufficient, since T_{90}, i.e., the temperature exceeded in 90% of the tumor, is below 40 °C [4,18].

In the following, we report on three clinical approaches (mEHT, TTF and TheraBionic), which unequivocally demonstrate in our understanding that non-thermal effects should exist. No or incomplete thermometry was performed in the outlined studies. Clinically experienced users of hyperthermia know, however, that with the low power levels applied (as listed below), temperatures high enough for any relevant thermal effect could never be reached.

3.1. Clinical application of AM-RF-HT at 13.56 MHz

Szasz et al. [28] provided a summary of the clinical evidence for use of AM-RF-HT, also referred to as mEHT. However, only a few clinical reports are suitable for evaluating the effect and significance of AM-RF-HT. Most notably and very instructive is a randomized study applying AM-RF-HT against cervical cancer [23]. The authors used the AM-RF-HT system, which is basically, a CS, and applied a remarkably low total power of 130 W without conducting any temperature measurement. Lee et al. [29,30] conducted a study on recurrent cervical cancer, utilizing AM-RF-HT with even slightly higher power of 150 W and measured temperatures in and around the cervical tumor, recording a mean temperature of 38.5 °C (38–40 °C). Thus, we estimate similar or even lower tumor temperatures in the above study that are not efficient in the sense of conventional hyperthermia.

Minnaar et al. achieved enhanced radiochemotherapy efficacy by the inclusion of AM-RF-HT, resulting in minimal cost and effort (low resource setting) without increased toxicity. An additional analysis revealed that effective AM-RF-HT could be employed nearly independently of the body mass index with negligible toxicity [24]. Interestingly, FDG-PET revealed that the majority of patients manifested extrapelvic (mostly para-aortic) lymph node disease (~70%) and were included in the study, while the RT and AM-RF-HT fields were confined to the pelvis. In these patients, complete metabolic remission was significantly more frequent than that in the AM-RF-HT-group (24.1% vs. 5.6%), suggesting an abscopal effect. These clinical observations are consistent with preclinical studies outlined in the next Section 4.

In comparison, other positive randomized trials on cervical cancer and cRF-HT required significantly higher total power either utilizing the elaborate APA technology with a total power of 400–800 W [3,18] or capacitive technology without AM with a total power of 800–1500 W [4,5]. Recently, an extensive update of heating technology for cRF-HT has been provided [11].

Furthermore, three retrospective reports are of interest in the assessment of the potential of AM-RF-HT. Lee et al. [29,30] treated patients with pre-irradiated cervical cancer recurrences either with chemotherapy alone ($n = 20$, platinum-based with paclitaxel or 5-FU) or chemotherapy plus AM-RF-HT for 60 min three times each week for a total of 36 sessions in 12 weeks ($n = 18$). The last follow-up demonstrated a significantly improved response in the AM-RF-HT-group [50% complete response (CR), 10% partial response

(PR), 10% stable disease (SD), 30% progressive disease (PD) versus 15% CR, 15% PR, 5% SD, 65% PD, $p = 0.0218$]. Both groups were well balanced according to age, FIGO stage, pathology, and recurrent lesions.

Fiorentini et al. [31] applied AM-RF-HT monotherapy to 28 patients with recurrent glioblastoma multiforme (GBM) and 22 patients with recurrent anaplastic astrocytoma (AST) who relapsed after standard first-line treatments (surgery, adjuvant radiochemotherapy and TMZ) [32]. The remaining patients in this retrospective observational multicenter cohort-controlled study (83 GBM, 14 AST) received best supportive care (BSC), including dexamethasone and palliative chemotherapy in 28 patients with GBM. Tumor response after 3 months (CR + PR + SD) was significantly higher in the AM-RF-HT group, i.e., 72% (AST) and 54% (GBM) vs. 37% (AST) and 19% (GBM) in the BSC group. Even if we consider a selection bias in favor of patients with AM-RF-HT, we must consider 10/22 objective responses (2 CR and 8 PR) in the AM-RF-HT group with AST (41%) and 7/28 objective responses (1 CR and 6 PR) in the AM-RF-HT group with GBM (25%). Apparently, a mean of 22 (range 11–62) AM-RF-HT sessions alone (150 W for 60 min after a step-up power protocol) can bring about relevant tumor regression. Questions remain due to the retrospective nature of this analysis (patient selection bias) as well as accurate measurement of brain tumor progression using brain MRI (true vs. pseudoprogression).

In the third study, Hager et al. [33] applied AM-RF-HT (70–150 W, 60 min) in 80 patients with liver metastases of far advanced stages of colorectal cancer and retrospectively analyzed the results. For all patients, they started with one course of 8 AM-RF-HT biweekly (without chemotherapy) in the liver and found an overall biochemical response (CEA and CA-19-9 decreased below 75% of initial values) in 25% of the patients. A total of 50/80 patients received only AM-RF-HT, whereas 30/80 patients later received chemotherapy (mytomycin + 5-fluorouracil + folinic acid) during the follow-up period. The authors reported remarkable survival times and objective tumor regression (CT-scans, ultrasound) in these patients. Again, AM-RF-HT alone appeared to cause significant tumor regression.

No firm conclusions can be drawn due to the retrospective design of the above studies. However, the clinical data suggest that AM-RF-HT at moderate temperatures $<40\,^{\circ}C$ should have non-thermal effects on various tumors.

3.2. Clinical applications of RF-EMF in the intermediate-frequency range 100–300 kHz

RF-EMF in the intermediate-frequency range 100–300 kHz, also known as tumor-treating fields (TTF), was first studied in patients with recurrent GBM and then clinically validated as an additional modality in first-line GBM treatment [25,32]. Treatment was delivered through four transducer arrays with nine insulated electrodes placed on the shaved scalp according to the planning software [34]. TTF was started 4–7 weeks after the end of simultaneous radiochemotherapy (e.g., together with the TMZ maintenance therapy) and was run every day for at least 18 h for a maximum duration of 24 months. The median survival was significantly improved from 16 months (TMZ alone) to 21.9 months in the TTF experimental group ($p < 0.001$). SAR or E-field distributions in the brain were calculated using the finite-element method [35,36]. Ballo et al. [37] used the Sim4Life quasi-electrostatic solver to ascertain E-field or SAR distributions and verified an association of overall survival and TTF E-field strength, achieving a better outcome for mean E-field strength >100 V/m. The SAR varied in the range of 0.3 to 3.2 W/kg that is not sufficient for any anti-proliferative thermal effect. Even though preclinical findings, dose-response relationships, and clinical outcomes of the study were consistent, the results were called into question. We note that the patients from the experimental treatment group are likely to have received superior medical care, as they were treated mostly within tertiary referral centers, which might also improve overall survival [38]. Furthermore, the long-term and nearly permanent wearing of the "electric hood" is associated with severe restrictions for the affected patients, which limits the quality of life of patients. In addition to newly diagnosed and recurrent glioblastoma, various other oncological applications of TTF are being studied, such as brain metastases, lung cancer, malignant mesothelioma, pancreatic cancer, HCC and ovarian cancer (www.novocuretrial.com). Mun et al. [39] referred to TTF as the fourth modality in cancer therapy and further described the potential for clinical applications on the head, thorax and abdomen. An indisputable advantage of TTF is its applicability to large anatomical regions throughout the human body, while a disadvantage is a need for permanent and long-term exposure to TTF.

3.3. Clinical application of AM-RF at 27.12 MHz

Clinical experience with AM-RF at 27.12 MHz, also referred to as the TheraBionic device, is limited to a few case series where the treatment was applied alone in advanced cancer. Barbault et al. [26] described the identification of tumor-specific AM frequencies using a simple RF generator at 27.12 MHz that powers an intrabuccal spoon-shaped applicator. The maximum SAR deposited in the body was estimated to be below 2 W/kg. Therefore, temperature increases in any tissue or tumor are negligible. AM is possible between 0.01 Hz and 150 kHz with a modulation depth of 85%. Variations in the radial pulse amplitude are claimed to indicate a tumor-specific AM frequency, which seems surprising. However, Sharma et al. [40] recently explained that the Ca^{2+} channel CACNA1H might be expressed in tumors and small vessels (endothelial and smooth muscle cells) that could affect the pulse amplitude.

In a total of 163 patients with various cancers, Barbault et al. discovered 1524 modulation frequencies between 0.1 and 114 kHz using their bio-feedback technique [26]. HCC, pancreatic cancer, ovarian cancer, BC and prostate cancer commonly exhibited frequencies between 1.8 and 10.5 kHz. Typically, more tumor-specific frequencies were found in advanced and progressive tumors. A total of 28 patients with advanced cancer received a low-level AM-RF at 27.12 MHz,

which implies a self-administered treatment of 60 min, three times a day for a mean treatment duration of months (range, 1–50.5 months). For 7/28 patients (25%), complete remission (1/28), partial remission (1/28) or stable disease (5/28) were documented according to the RECIST criteria. These findings suggest non-thermal therapeutic effects of AM-RF with tumor-specific AM frequencies.

Costa et al. [27] conducted a phase I/II study in 41 patients with advanced HCC, who had either failed standard therapy or had severely impaired liver function limiting any kind of systemic treatment, and used AM-RF at 27.12 MHz as monotherapy. Of these patients, 4/41 had partial remission and 16/41 stable disease for $\geq$12 weeks (49% long-term control), with 4/41 patients becoming long-term survivors (>3 years). These data confirmed the potential of using AM-RF at 27.12 MHz.

4. Preclinical studies

Numerous preclinical studies have investigated the non-thermal effects of EMF. Investigations mainly dealt with the possible risks of EMF at low levels without a relevant temperature increase. Epidemiological studies [41,42] have focused on EMF either in the extremely low-frequency range (ELF; <3 kHz) or in the RF-range (3 kHz up to 300 GHz). EMF exposure at ELF is ubiquitous and is mainly caused by electric lines and associated grounding systems, while wireless communication applications are the source of RF exposures. Organizations such as the World Health Organization and the International Commission of Non-Ionizing Radiation Protection stated that although epidemiological studies have suggested links between EMF exposure and health effects, they could not provide a reliable interpretation [43–46].

Forschungsgemeinschaft Funk thoroughly examined the possible non-thermal effects of weak EMF (http://www.fgf.de/index2.html) from 1992 to 2009 in Germany and published the results in 2009. The REFLEX (Risk Evaluation of Potential Environmental Hazard from Low Energy Electromagnetic Field Exposure Using Sensitive *in vitro* Methods) study was an elaborate European union (EU) project from 2000 to 2003 involving 12 research groups from seven countries. Standardized exposure systems for EMF magnetic fields [47] and RF exposures at 900 MHz [48] and 1800 MHz [49] were constructed according to development guidelines [50]. Nevertheless, the results were highly controversial and not reproducible, indicating the difficulties in obtaining clear conclusions in this field of research.

In the actual extensive "Handbook of Biological Effects of Electromagnetic Fields" (two volumes with 1150 pages) the technical term "non-thermal" is not even mentioned [51,52] but the issue was discussed as controversial [53,54].

In the previous Section 3, we listed recent clinical studies (mEHT, TTF and TheraBionic) that strongly suggest the existence of non-thermal effects. As a result, we focused on the associated preclinical investigations, which have provided the prerequisites for these clinical applications. It is precisely this recent clinical and preclinical work that is most likely to contribute to the controversial discussion.

The biological endpoints of cells or animal tumors are an important issue. Clearly, the clonogenic assay is the gold standard if radiotherapy dosages or thermal doses are directly transferred to the clinics. However, the question here is whether there are non-thermal effects and which mechanisms are underlying. Then other biological endpoints than clonogenicity are also of interest, e.g., apoptosis, damage-associated molecular pattern (DAMP) and others. In spite of the huge number of literatures on this issue, we are not at the point to formulate a dose concept for non-thermal effects.

4.1. Amplitude-modulated (AM)-RF-HT at 13.56 MHz

Figure 1 depicts the experimental setup for evaluating the biological effects of AM-RF-HT on cell suspensions as the preclinical counterpart of mEHT or oncothermia; the findings can easily be compared to the effects of WB-HT [55,56]. In parallel to the clinical application, the RF source generates a carrier frequency of 13.56 MHz with an adjustable AM starting at a given minimum modulation frequency *f* and then declining with *1/f* (pink noise) with a selected modulation index *m* (LabEHY-200, Oncotherm Kft., Budapest, Hungary) as described in detail in [57]. Temperatures are typically measured in the center of probes of <1 ml (dimensions <1 cm) and in the surrounding distilled water by fluoro-optic sensors. Then the probe temperature represents the maximum temperature and is controlled by the RF power. Temperature deviations in the probe of a few tenths of a degree are possible but are further reduced if the surrounding water is warming up near to the probe temperature. However, the crucial parameters SAR or E-field in the specimen are not always clearly defined in preclinical studies with this applicator (see Figure 1 legend). SAR can be determined by measuring the rate of temperature increase over time (°C/min).

The bioheat-transfer equation predicts SAR of 200 – 300 W/kg to heat a sphere of 1 cm diameter from 37 °C to ≈42 °C. The SAR declines below 100 W/kg when the ambient temperature rises above 40 °C [58]. That is the typical

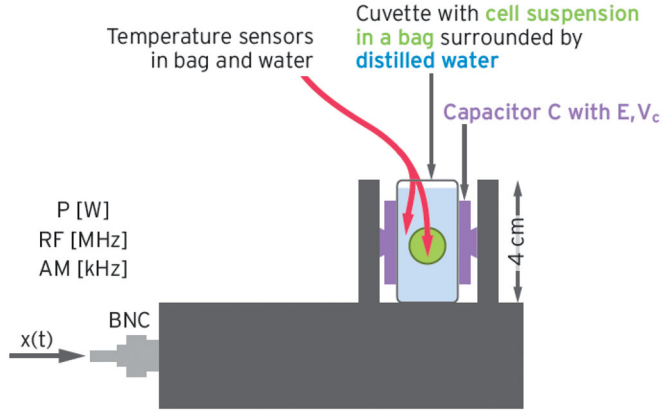

Figure 1. Design of an experimental setup to expose a cell suspension (green) to AM-RF-HT [55]. A mean E-field emerges between the electrodes of the capacitor *C* generated by the voltage V_C. The capacitor *C* in series with an inductivity *L* (with loss resistance *R*) establishes a resonance circuit with resonance frequency RF [56]. It is desirable that temperature *T* (set and maintained using a flow system) and SAR (set by V_C) can be selected separately. If the resonance condition $f = 2\pi(LC)^{1/2}$ is met, the system is well matched, i.e., in resonance.

description of an experiment according to Figure 1—not far away from the clinical situation [55]. The formation of selective small-volume overheating in regions of approximately 1 mm extension would require excessive SAR > 10,000 W/kg or even SAR >1,000,000 W/kg for areas of 0.1 mm extension etc. —as outlined in a series of publications about point heating or nanoheating [58–62]. We note that a simple arrangement of a 1 ml cell suspension in a capacitor cannot generate such high SARs that would be required to generate hot spots on a microscopic level.

Another arrangement is applied for *in-vivo* experiments with mice tumors. Here, an electrode of 1.8 cm diameter is positioned on tumors of a few millimeter size with a neutral electrode on the opposite. As illustrated by [63] SAR between 100 – 400 W/kg are generally required to heat such small tumors to 40 – 42 °C in accordance with our own experience (unpublished results).

Obviously, in case of mEHT, the preclinical studies use 10 times higher SARs than clinically attainable resulting in only 3 times higher E-field strengths. Higher electric field strengths can facilitate the detection of non-thermal effects and lead nevertheless to valid results if relevant thermal effects can be excluded.

The data show higher rates of apoptosis for AM-RF-HT (typically 42 °C for 30–60 min) in comparison to standard WBHT at the same temperature [64]. The greater effectiveness of AM-RF-HT compared to infrared (IR) HT for nude mice xenografts *in vivo* [65] or WBHT for cell suspensions (human cancer cell lines) *in vitro* [66–68] has been demonstrated by microscopic detection of dead cells or apoptotic cell death. A 30 min treatment with AM-RF-HT at 42 °C was 3.2-fold more effective than IR-HT at 42 °C. Notably, 30 min of AM-RF-HT at 38 °C was still 2.6-fold more effective. In cell suspensions, the apoptosis-inducing effect of AM-RF-HT at 42 °C was similar to that of WBHT at 46 °C. Apoptosis was associated with increased caspase activation, calreticulin expression, and intra-/extracellular HSP70 expression. Andocs et al. [69] found a complex dependency of AM-RF-HT efficacy on temperature, i.e., increased efficacy from 39 °C to 42 °C (45% dead cells) and then a (slight) decrease at 43–44 °C (30% dead cells) suggesting that for temperatures <43 °C, AM-RF-HT generates considerably more dead cells than WBHT, although the temperature dependency for AM-RF-HT and WBHT might be different.

Several preclinical studies employed 1–3 sessions of AM-RF-HT (42 °C, 30–60 min) and measured the apoptosis rate in xenografts and/or tumor cell suspensions [66,70–76]. Researchers consistently found high rates of apoptosis—which were markedly higher than those expected for traditional heat treatment at 42 °C—in comparison to the control groups. Further, several indicators of cellular stress, such as elevated HSP70, calreticulin, HMGB1 and damage-associated molecular pattern (DAMP) signals are associated with AM-RF-HT alone [63,72,75,77]. AM-RF-HT induced significantly higher HSP-levels than WBHT at the same temperature [67]. It is known that DAMP signals can support immunogenic cell death (ICD) in response to chemotherapy, radiotherapy, immunotherapy or immune checkpoint inhibition therapy [78,79]. In fact, for symmetrical tumors (both femoral legs in mice), treatment-related effects were also observed in untreated tumors (compared to the sham controls) [75,80]. In a CT26 murine colorectal cancer model, Tsang et al. [66] found a synergism between intratumoral dendritic cell injection and AM-RF-HT, and a systemic effect (prevention of contralateral tumor seeding). Thus, AM-RF-HT can support local and systemic ICD-mediated tumor killing. The abscopal effects of AM-RF-HT were clinically confirmed [23].

Combination treatment of AM-RF-HT and RT [81–84] was found to result in greater tumor damage, particularly if AM-RF-HT was immediately—or at least within 4 h—followed by RT in fibrosarcoma allografts (in C3H mice) and various cancer cell lines (9 L, MCF-7, Panc-1). Interestingly, the opposite order (RT followed by AM-RF-HT), which is common for cRF-HT, was less effective.

AM-RF-HT has been used in combination with chemotherapeutic agents. The cytotoxic effect of doxorubicin was potentiated when doxorubicin was preceded by two 30 min treatments of AM-RF-HT at 42 °C [76]. In another study, cancer cells (HepG2, A 549, U87MG and CT26) were treated with liposome-encapsulated doxorubicin (Lipidox®, Stockholm, Sweden) and then subjected to WBHT (42 °C, 30 min) or AM-RF-HT (42 °C, 30 min) [85]. Lipidox® plus AM-RF-HT exhibited higher cytotoxic effect (viability 10–20%) than Lipidox® plus WBHT (50–75%) and Lipidox® at 37 °C (80–95%).

Interestingly, most available references do not specify the parameters of the AM (*f* and *m*) adjusted for the AM-RF-HT. We determined a typical default setup in the clinical device EHY 2030, amounting to $f \approx 60$ Hz and $m = 0.2$, and comparable parameters are assumed for the preclinical devices (own unpublished measurements). Wust et al. [55] detected already for RF-HT (without additional AM) more antiproliferative effects than those in WBHT (80–100% vs. 45–50% clonogenicity in HT-29 and SW480 cells). This is in line with our experiences with cRF-HT. The importance of any type of AM is currently under investigation. It should be noted that different biophysical mechanisms may underlie RF- or AM-RF-induced non-thermal effects (see below).

4.2. RF-*EMF in the intermediate-frequency range 100–300 kHz*

Pairs of insulated wires or electrodes are suitable for generating low-intensity RF-EMF of 100–300 kHz in cell cultures or tissues. *In vitro* studies on eleven different types of cancer cell lines and *in vivo* studies on mice tumors showed arrested proliferation, cell destruction, and reduction in tumor growth [86]. A 24 h exposure of EMF with moderate strengths of 100–140 V/m (comparably low SAR of approximately 5–10 W/kg without considerable temperature elevation) resulted in a significant decrease in growth rate (relative to that of the control) of 10–90% depending on the cell line. This application was labeled as tumor treating fields (TTF). Antiproliferative effects increased with E-field strength and depended on frequency and cell line (e.g., maximum for B16F1 cells at 120 kHz and F-98 cells at 170 kHz). Kirson et al. [86] identified two E-field effects, which are not temperature-

dependent. First, the E-field polarizes and orients tubulin dimers and other charged macromolecules in the direction of the E-field during the early phases of mitosis, which interferes with proper chromosome alignment and separation. Second, during cleavage, the E-field is strongly inhomogeneous, exerting an electric force on all intracellular charged and polar macromolecules. Since dividing cells are disturbed and sometimes destroyed, the authors suggested a novel treatment modality for cancer. Another paper extended the investigations to additional cell lines and animal tumor models [87]. The combination of chemotherapy (paclitaxel, doxorubicin, and cyclophosphamide) with TTF resulted in strong sensitization [88]. Silginer et al. [89] supplemented preclinical information for several glioma cell lines and identified 100 kHz as the most effective frequency for glioma. TTF also hampered the invasiveness and migration of glioma cells. Importantly, glioma cells responded to TTF independent of MGMT status and/or TMZ resistance.

4.3. AM-RF *at 27.12 MHz*

Barbault et al. [26] exposed cancer patients to low-level AM-RF (<2 W/kg) with a carrier frequency of 27.12 MHz and selected modulation frequencies from 0.01 Hz to 150 kHz with a high modulation index of 0.85, which does not cause any temperature increase. This system is also referred to as TheraBionic™ (Ettlingen, Germany). The authors briefly described a bio-feedback method (measuring skin electrical resistance, pulse amplitude, and blood pressure) and identified a variety of cancer-specific modulation frequencies (see also [90]). This low-level AM-RF was evaluated in three preclinical studies.

Zimmerman et al. [91] utilized cancer-specific modulation frequencies identified in hepatocellular carcinoma (HCC) and breast cancer (BC) cell lines. They described the antiproliferative effects associated with changes in gene expression in two representative HCC cell lines (HepG2 and Huh7) exposed to AM-RF for 21 h in seven days (3 h per day) or longer with HCC-specific AM frequencies. A commonly used tritium incorporation assay determined the growth inhibition that persisted over a period of seven weeks. We highlight some interesting results of this early preclinical study. First, significantly lower growth inhibition was measured using randomly chosen (non-specific) or BC-specific AM against HCC cells, instead of HCC-specific AM. Second, HCC-specific AM did not affect the proliferation of BC cells (here MCF-7) or normal hepatocytes (THLE-2). Third, within the entire SAR range (from very low levels of 0.05 to 1.0 W/kg), they measured significant antiproliferative effects. Fourth, growth inhibition depended on the exposure time. They did not observe any effect for reduced exposure times such as 1 h per day for seven days or 3 h per day for three days but achieved the same level of effect for longer exposure times such as 6 h per day for seven days. Application of HCC-specific modulation frequencies for more than 21 h resulted in mitotic spindle disruption in more than 60% of HCC cells. Therefore, for both approaches (TTF and TheraBionic), a minimum exposure time was required to achieve a significant antiproliferative effect but this effect did not always increase with prolonged exposure time.

These results were confirmed and explored in two recent studies. Jimenez et al. [92] exposed additional HCC cell lines (HepG2, Hep3B, Huh7, HCCLM3 and MHCC97-L) to the same AM-RF (27.12 MHz with low SAR between 0.03 and 0.4 W/kg) for 3 h daily for seven days. They found antiproliferative effects only for AM-RF with HCC-specific AM. Interestingly, growth inhibition was associated with increased intracellular Ca^{2+} resulting from Ca^{2+} influx through a special T-type low voltage-gated Ca^{2+}-channel (VGCC) CACNA1H [93–95], which appeared to be selectively sensitive to HCC-specific modulation frequencies. *In vivo* experiments with mice carrying human HCC xenografts confirmed the inhibition of tumor growth by AM-RF exposure with HCC-specific AM.

Sharma et al. [40] described the same pattern for human BC cell lines (T47D, BT-474, SKBR3, MDA231 and MDA-MB-453) with different BC-specific AM. Additionally, after intracranial injection of HER2-positive or triple-negative BC cells into SCID mice, the implanted brain metastases were exposed to AM-RF with the same low SAR (0.03–0.4 W/kg) 3 h each day until the experimental endpoint. For both cell types, they found significant suppression of metastases and tumor growth, resulting in significantly improved brain metastasis-free survival. Again, AM-RF-EMF with BC-specific frequencies in BC cells was associated with increased Ca^{2+} influx through the same CACNA1H channel. However, an exact biophysical mechanism has not yet been described.

5. Model approaches to describe non-thermal antiproliferative effects

Biophysical mechanisms were not presented to the best of our knowledge until now to explain the controversial non-thermal effects, in particular, in the clinically relevant RF range from 1 to 150 MHz. This lack of theory building is a common argument against the existence of non-thermal effects. In fact, works that refute the existence of non-thermal effects are predominantly of a theoretical nature [43,44,46,96–100]. How else can you deal with something that does not exist?

Predominantly in past experiments, higher frequencies (microwaves up to terahertz) were investigated with regard to their non-thermal resonance effects [101,102]. Therefore, theoretical considerations mentioned above have attempted to refute such resonances in macromolecules, e.g., DNA or enzymes [44,97–99,103]. These high frequencies (>300 MHz) are, however, of minor importance for clinical hyperthermia because of their limited penetration depth.

In the following section, we focus on the membrane effects of EMF in the lower RF range (<100 MHz).

5.1. Nanoheating

The term nanoheating (formerly known as point heating) refers to the deposition of a very high SAR in a microscopic volume, e.g., a protein cluster (nm to μm size) in the cell membrane or the cytoplasm. This theoretically fascinating therapeutic approach occupied many researchers in a series of publications, beginning at the time of World War II

[58–62]. The underlying problem can be solved by an analytical solution of the partial differential equation for the temperature distribution, which ultimately represents a diffusion equation with a transport term (perfusion) known as the bioheat transfer equation. In the cited works it was consistently shown that a circumscribed SAR increase in regions <1 mm must be unrealistically high in order to generate a thermal effect (e.g., SAR > 10,000 W/kg for a 1 mm sphere). On the other hand, with realistic SAR increases, only minimal temperature increases of fractions of 1 °C are expected. In conclusion, non-thermal antiproliferative effects, at least in part, must exist to explain preclinical and clinical data.

Nanoheating is specially investigated after the administration of nanoparticles in the target and exposure to an alternating magnetic H-field [104–106]. Analysis of available ferrofluids and tolerated H-fields (frequency and amplitude) shows that effective heating of lesions <1 cm is difficult. Thus, nanoheating, without nanoparticles, appears even more difficult.

Based on current technology, typical incident E-field intensities under clinical conditions are in the range of $E = 50–350$ V/m corresponding to SAR = 1–60 W/kg. Uncomplicated and cost-effective devices achieve a low SAR of 5–15 W/kg ($E = 100–170$ V/m). These E-fields are negligible compared with the E-fields between the inner and outer surfaces of the lipid bilayer of $E > 10^6$ V/m associated with the resting potential of approximately 30–100 mV at membranes of 4–5 nm thickness. However, the distribution of electrical constants such as the relative permittivity ε_r and conductivity σ (in S/m) is inhomogeneous in living tissues and might generate higher E-fields caused by electrical boundaries compared with the incident E-field [107]. The field distribution is determined by solving Maxwell's equations, which is certainly a challenge at the microscopic level. In particular, Maxwell's 4th equation causes elevations of E at the electrical boundaries.

Eibert et al. [108] investigated this issue and performed an electromagnetic and thermal analysis of an exposed structure depicted in Figure 2. They showed that with such arrangements, voltages of a few millivolts arise on and in the membrane, which is in the percentage range of the resting membrane potential. In Figure 2, the electrical constants ε_r and σ are taken for the frequency range of ≥70 MHz.

Figure 3 schematically shows the frequency-dependent behavior of ε_r in living tissues [109,110], indicating the range of cRF-HT with $\varepsilon_r \sim 80$ (above 70 MHz). The so-called δ-dispersion formed by proteins, protein-bound water and organelles [110] leads to this well-known plateau representative of APA technology (70–120 MHz). However, the δ-dispersion also causes a 10-fold higher ε_r of ~1000 at 10–30 MHz (of AM-RF), while the α- and β-dispersions result in a 1000-fold higher $\varepsilon_r > 100{,}000$ at intermediate frequencies (100–300 kHz). Such a high ε_r might create a large E of 500 V/m (corresponding to local SAR of 120 W/kg) in certain microscopic areas (as shown in Figure 2) if the AM-RF-HT-technique at 13.56 MHz is applied (or other CS around 10 MHz). This fact might partially compensate for the technological advantage of the APA technique at RF around 100 MHz.

In the intermediate-frequency range, local E-field peaks along the membranes can be large (~100,000 V/m) in addition to the described specific mechanisms during cell division. This might be a further explanation for the effectiveness of RF-EMF in the intermediate-frequency range.

Papp et al. [111] investigated the power absorption in transmembrane protein clusters (rafts) with an assumed diameter of 1 μm and enhanced permittivity and conductivity in comparison to the adjacent membrane layer. They created a 3D model of the raft embedded into the membrane and simulated the E-field distribution using CST EM Studio (Computer Simulation Technology software, Darmstadt, Germany). Assuming realistic excitations of 100 V/m E-field elevations up to 300 V/m (SAR of 40 W/kg) occurred at the

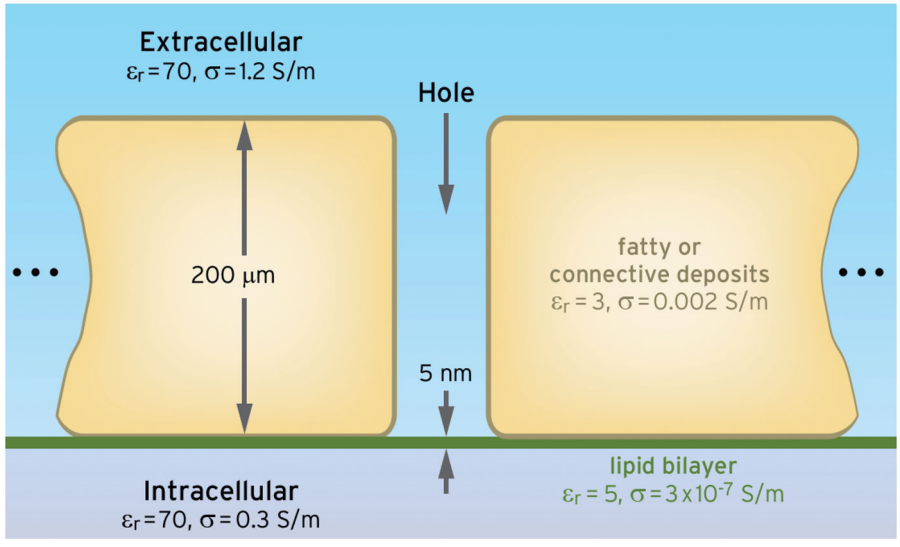

Figure 2. Three-dimensional configuration analyzed by Eibert et al. [108] using sophisticated numerical methods. They found for this special arrangement that the high electrical jump between the extracellular fluid ($\varepsilon_r = 70$, $\sigma = 1.2$ S/m, blue) and fatty or connective deposits ($\varepsilon_r = 3$, $\sigma = 0.002$ S/m, yellow) cause high E-fields of some 1000 V/m (and SAR of 500 W/kg) at a lipid bilayer (membrane) between. Voltages as high as millivolts can be generated in these membrane sections. This analysis is valid for $RF > 70$ MHz (see dispersion curve in Figure 3).

rafts and are probably of minor effect. We note that the authors [111] assumed a much higher excitation of 50,000 V/m and resulting SAR peaks that are clinically unrealistic.

In summary, current theoretical approaches do not indicate that energy transfer by EMF to biological macromolecules can disturb their function or even cause chemical conversions.

5.2. Biophysical processes on transmembrane ion channels

Preclinical and clinical experience with AM-RF-HT at 13.56 MHz and AM-RF at 27.12 MHz suggest that non-thermal mechanisms exist, which stress and finally damage the exposed cells. Suitable AM might enable or at least enhance these processes. The non-thermal effects of AM-RF could arise from electrical disturbances at the membranes. Therefore, we examined the ion channels more closely.

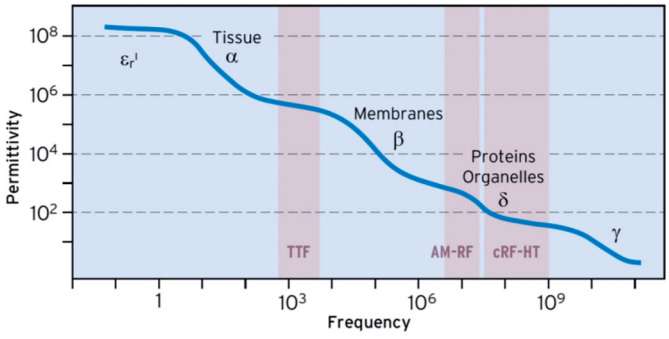

Figure 3. Frequency dependency (dispersion) of permittivity ε_r. The plateau with $\varepsilon_r \sim 80$ characterizes the conventional RF-HT for APA technology (50 MHz to GHz). The δ-dispersion causes much higher ε_r of $\approx$ 1000 at 10 MHz in favor of the capacitive technology. In the TTF range of some 100 kHz $\varepsilon_r >$ 10,000 at arrangements of macromolecules, which might induce huge E-fields under special conditions (see Figure 2).

We validated the non-thermal effects of RF at 13.56 MHz without AM in a typical preclinical experiment using LabEHY-200 [55]. For a better understanding, we developed a model for ion channels based on textbook knowledge [112–115]. Figure 4 shows an example of a Ca^{2+} channel, which was proven to be particularly important for non-thermal effects. This model is also extrapolatable to potassium (K^+), sodium (Na^+), chloride (Cl^-) or hydrogen (H^+) ions. The basic elements of a typical ion channel are the entrance (here outer) pore, which has a mechanism for opening and closing (gating) with some selectivity for the particular ion (here Ca^{2+}), a cavity to collect the ions, and the selectivity filter as the most important and highly specific part for the particular ion. The ion gains the dehydration energy by a specific chemical reaction with carbonyl oxygen atoms lining the selectivity filter, stalls in the filter, and can only exit by exploiting electrostatic repulsive forces if the next ion enters from the cavity [112].

We assume that every channel act like a diode because ions can only be directed along the electrochemical gradient. Our example (Figure 4) shows a huge Ca^{2+} gradient between the extracellular concentration of 1.3 mmol/l and intracellular concentration of only 100 nmol/L (>10,000-fold). Then, the equilibrium (Nernst) potential for Ca^{2+} is $U_{Ca} \approx 250$ mV, which is far from the typical membrane potential of –60 mV. This electrochemical gradient is enormous, causing a strong tendency for calcium influx and intracellular calcium overload if the calcium channel is open. Instead, in the case of potassium, the K^+ equilibrium (Nernst) potential of $U_K = -95$ mV is below the membrane potential of 60 mV. Therefore, K^+ ions flow from intracellular to extracellular to bring the membrane potential nearer to the K^+ equilibrium potential. Thus,

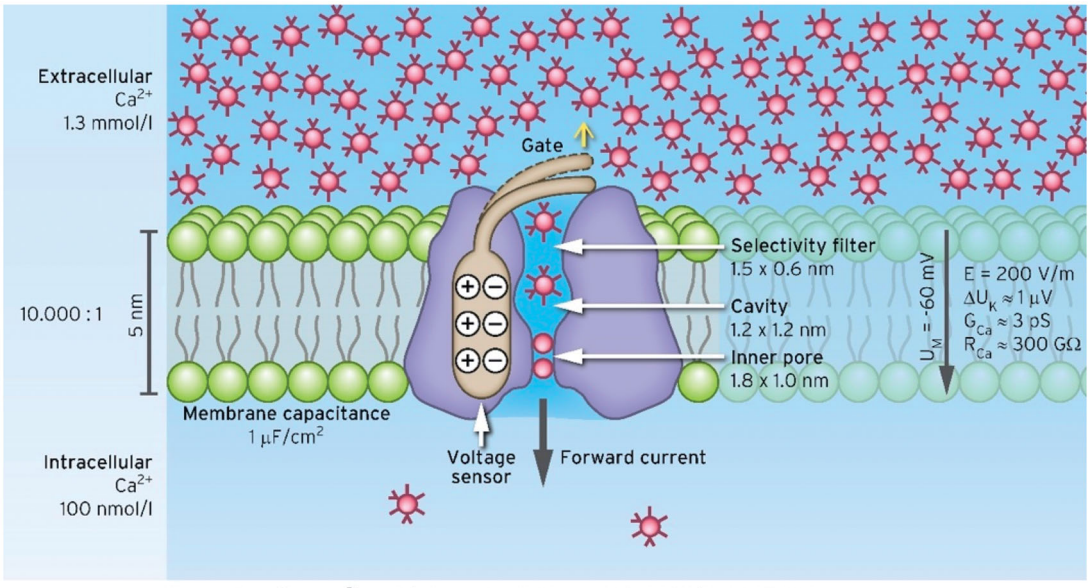

Figure 4. Model of a calcium channel to estimate R_{Ca} and G_{Ca} that we used as a template for ion channels [112]. The ion channels act like diodes with forward direction along the electrochemical gradient (for calcium from extra- to intracellular). The selectivity filter is magnified for clarification. There is a large electrochemical gradient toward intracellular due to the difference between the membrane potential of -60 mV and the Ca^{2+} equilibrium potential of 250 mV. High concentration gradients >10,000 predispose cells to excessive calcium influx. Thus, disequilibrium of intra-/extracellular calcium concentrations is more probable for calcium than for other electrolytes.

a potassium channel acts like a diode with the forward direction from intra- to extracellular.

The resistances of ion channels can be estimated using basic electrical principles (e.g., $R_{Ca} = 323\,G\Omega$ or $R_K = 4.3\,G\Omega$, see [55]) and the surrounding membrane contributes a capacitance C. Figure 5 (right) shows the equivalent circuit diagram, which is basically a diode in series with a low-pass filter RC (with resistance R and capacitance C). Thus, the voltage associated with the RF E-field along the channel (i.e., perpendicular to the membrane), is rectified and smoothed. In the case of a pure sinusoidal RF wave ($E = 200$ V/m assumed), a direct voltage of $\sim 1\,\mu V$ is emerging (see dotted line). Additional AM with a single modulation frequency, after demodulation, yields the solid sinus curve overlaying this direct voltage. Direct voltage and superimposed alternating voltage might exert different effects on the channel (see below). In certain regions with electrical inhomogeneities, E-fields can be higher (see the previous section) and the generated direct voltage can approach the millivolts range under special conditions (Figure 2) [108].

While the ion flux through a single channel caused by some microvolts to millivolts might be considered ineffective, a mean channel density of 1 channel/μm^2 (i.e., 2000 channels in the membrane that point in the direction of the E-field) and an exposure time of 30–60 min (1800–3600 s), can enhance the stress on the cell by a factor $>10^6$. This contrasts with the fact that the channels are often (but not always) closed.

Even such a small voltage offset of 1 μV along >1000 ion channels for >1000 s will cause a relevant disequilibrium of ions in the affected cells, which can be much higher than the complete ion content for sodium, chloride, and protons and >100-fold larger than the intracellular calcium content. Table 1 (1st column) shows the relative intracellular ion increase resulting from Ohm's law. However, it is supposed that mostly, fast chemical reactions control the flux through the ion channel (facilitated diffusion), which considerably accelerates the exchange (2nd column). A DC voltage of 1 μV (or the associated E-field of 200 V/m) causes a drift velocity v_X of the ion X. Then, we estimate the maximum flux through the selectivity filter dividing v_X by the hydration diameter d_X, if we assume that the ions pass the channel (and, in particular, the filter) in a single file with maximum rapidity. Wust et al. [55] provided further details of the models, basic equations, and calculations.

Table 1 summarizes the results and suggests that increased intracellular Ca^{2+} most likely explains non-thermal damage to cells. Indeed, researchers reported increased intracellular calcium in association with non-thermal antiproliferative effects of AM-RF-HT [68], AM-RF at 27.12 MHz [40,92], and RF-EMF in the intermediate-frequency range [116]. Researchers identified VGCC of the T-type CACNA1H (in HCC or BC) or L-type CACNA1C (glioblastoma) as sensitive to EMF used with AM-RF at 27.12 MHz or RF-EMF in the intermediate-frequency range and causal for intracellular Ca^{2+}

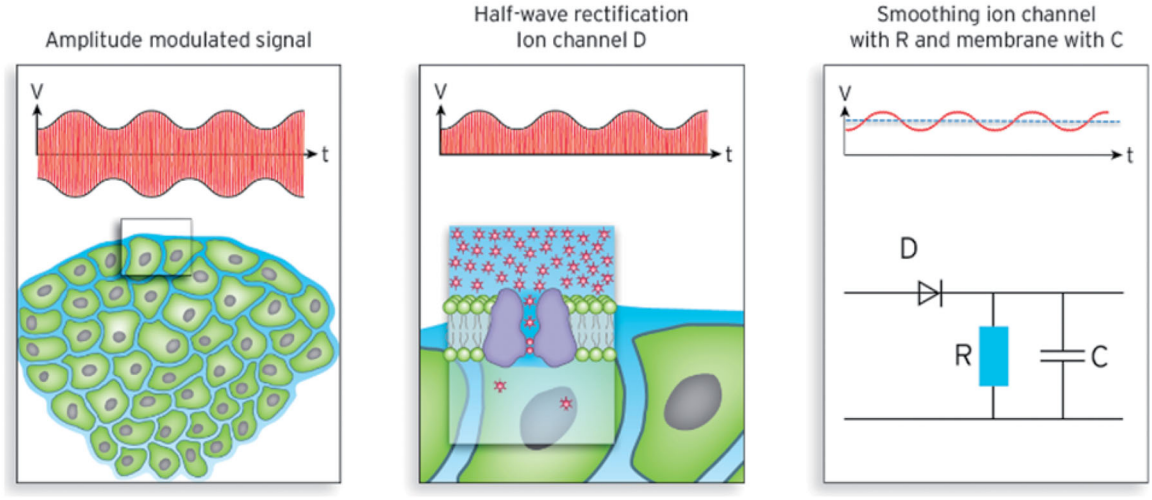

Figure 5. Left: Typical tumor environment characterized by isolated tumor cells surrounded by extracellular water. Middle: Simplified model of ion channels in the membrane (e.g., potassium) showing the internal pore, cavity and selectivity filter. This model is an archetype for other ion channels. Right: Equivalent circuit diagram of an ion channel according to the ion channel model of Figure 4. After rectification of the amplitude-modulated (AM) carrier radiofrequency (RF) (~10 MHz) a low-pass filter (specified by *RC*) generates a mean DC voltage (1 μV for SAR of 25 W/kg) with a superposed sinus oscillating with the modulation frequency in the kHz range (red solid line). For *RF* of 10 MHz the condition $RC \gg 10^{-7}$ s holds.

Table 1. Estimated fluxes through ion channels caused by 1 μV either derived applying Ohm's law or assuming maximal facilitated diffusion (passage in file) and their impact on ion imbalances assuming 1000 channels and 1000 s exposure time resulting in an enhancement factor 10^6. The highest imbalance is expected for Ca^{2+} (bold).

Ion X	Flux N_X(1 μV) [s^{-1}] Ohm's law	Max flux N_X(1 μV) [s^{-1}] v_X/d_X in file	Total ion content in cell	Relative ion loss/increase $10^6 \times N_X$/total cell content	Drift velocity v_X [μm/s]	Hydration radius d_X [nm]
K^+	1500 out	38,000 out	5×10^{10}	0.03–0.76	15.2	0.25
Na^+	300 in	20,800 in	2×10^9	0.45–10.4	10.4	0.35
Cl^-	1100 in	39,500 in	2×10^9	0.54–19.4	15.8	0.20
H^+	10^{-2} in	120,800 in	3×10^4	$0.4–5 \times 10^7$	72.5	0.60
Ca^{2+}	19 in	30,800 in	3×10^4	**>100–1600-fold**	12.3	0.30

overload. Pall et al. [117] listed 23 additional studies that demonstrated activation of VGCC by EMF of different kinds. Notably, one single open Ca^{2+} channel indicates that the RF enforces a calcium overload of the cell many times over the regular content with the preconditions of Table 1 (bottom line). Interestingly, T-type VGCCs require only a moderate depolarization of 10–20 mV for activation/opening [118] and are probably particularly sensitive to influences on the cell membrane.

An overload of intracellular calcium and protons and/or a decline in the intracellular pH will certainly harm the cell. Additionally, intracellular overload of NaCl may cause cell edema/swelling, leading to cell death, and intracellular loss of K^+ may promote apoptosis [119]. Ion channels provide the key to understanding the non-thermal effects, even though the exact biochemical mechanisms are unknown.

Abnormalities of ion channels in tumor cell lines have been described in numerous publications [119–126]. Ashrafuzzaman's textbook (Chapter 8) provides a summary [127]. In tumor cells, with increasing aggressiveness, certain channel families are often overexpressed, e.g., transient receptor potential (TRP) channels. They are responsible for calcium transport, proton transport (pH regulation), and water exchange (aquaporins). T-type calcium channels are broadly expressed in various malignancies [93]. Differences in ion channels (channelomes) in tumors and normal tissues can contribute to an increase in the therapeutic quotient. Both the duration and sequence play a decisive role in the non-thermal effects and may differ significantly from cRF-HT.

5.3. Frequency-dependent effects on cells

Frequency-dependent effects caused by particular modulation frequencies on an RF carrier were described by two research groups more than 40 years ago [128,129]. Both described a calcium release in brain tissue caused by AM-RF of 147 MHz with an ELF of 10–20 Hz at low intensities of ~1 W/kg; in a control without AM, they found no effect. Later, researchers described comparable effects in brain tissue exposed to ELF directly without a carrier [130] and noted its dependence on temperature [131]. These results are controversial [96,100,132–134]. We note that in some refuting studies pulsed microwaves were used, which is clearly not the same as AM-RF (see below).

An analysis of the experimental data reveals a non-thermal gain in effectiveness through AM of the RF with modulation frequencies hertz to 20 kHz (audio frequencies). Preclinical and clinical experience with the AM-RF-HT indicates effectiveness for lower AM frequencies in the range of 100 Hz to a few kilohertz considering the pink-noise approach, which typically starts at a minimum frequency of 100 Hz. Instead, experiences and data using AM-RF at 27.12 MHz predominantly indicate frequencies >1 kHz (up to 20 kHz). Increased efficacy with duration and number of applications is always observed.

For a reasonable explanation of the resonance frequencies generated by AM-RF-HT on cells (Hz–20 kHz), we refer to our model of an ion channel. Because the dehydrated ions are trapped in the selectivity filter, every periodic force is transmitted to the adjacent membrane. As depicted in Figure 6, the membranes consist of vibratory sheets or tiles, which are isotropic or at least six-fold symmetric. Such membrane

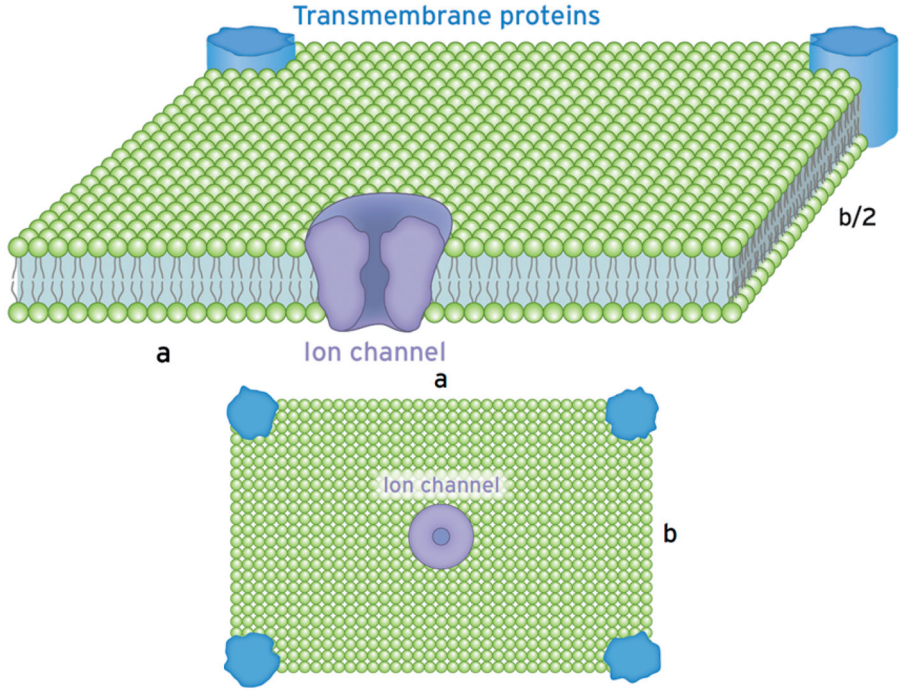

Figure 6. Schematics of a single section of the cell membrane that is excited by the ion channel to vibrate. This membrane section perpendicular to the incident wave behaves like a sheet $a \times b$ with supported edges. Such a vibratory structure can be excited to natural bending oscillations in the frequency range from hertz to kilohertz depending on the dimensions a, b and the stiffness of the membrane described by the Young's modulus Y (see text). Excitable tiles with larger extensions can be composed of these sections with an increased number of exciting ion channels. The Eigen frequency declines with increasing dimensions a and b, given in μm.

portions are characterized by only two elastic parameters [135,136]. The first parameter is the volume compression modulus K_V, which amounts to 10^7–10^8 Pa. These consistently high values of the compression modules for lipid bilayers and cell membranes reflect the incompressibility characterizing both solids and liquids [135]. The second parameter describes the fluidity (elasticity) of membranes and may vary considerably (see below). Poisson's ratio σ is a suitable parameter to describe fluidity. For $\sigma = 1/3$, the stiffness is high and describes a solid. Instead for $\sigma \Rightarrow 1/2$, the membrane increasingly takes on the properties of a liquid. The corresponding elasticity parameters are either Young's modulus Y (also called stiffness) or shear modulus μ (also called torsion). The basic relationships between elasticity parameters are derived according to [136 §5]:

$$Y\ [\mathrm{Pa}] = 3 \times (1 - 2\sigma) \times K_V$$
$$\mu\ [\mathrm{Pa}] = Y/(2 \times (1 + \sigma))$$

Both decline (and finally approach zero) in comparison to K_V as σ goes toward $1/2$.

Assuming the Young's modulus Y of a membrane section in Figure 6, the resonant frequencies for the bending vibration of this sheet with supported edges can be calculated accordingly [136, § 25]:

$$f\ [\mathrm{kHz}] = 120 \times Y^{1/2}\ (n/a^2 + m/b^2)\ ;\ n,\ m = 1,\ 2,\ \ldots \quad (1)$$

with Y in Pa, a and b in μm.

For $n = m = 1$, we obtain the fundamental oscillation and for $n, m > 1$ high-frequency harmonics.

For $Y = 500$ Pa and $a = b = 10$ μm, we calculated a fundamental resonant frequency $f = 53$ Hz assuming a vibration of the whole membrane face. If only parts of the membrane are excited, for example, $a = b = 1$ μm, we calculate $f = 2.7$ kHz. Depending on the stiffness Y [Pa] of the membrane and the extension a, b [μm] of the oscillating sheet, we predict the resonant frequencies in the hertz and kilohertz ranges that match the modulation frequencies used in the previous sections.

The mechanical properties of tumor cells and normal cells may strongly differ [137,138]. Generally, tumor cells are more deformable and elastic in correlation with higher adhesion, migration, invasiveness, and metastasis formation. Table 2 shows the upper lines for a typical $K_V \simeq 10^7$ Pa that theoretically, the calculated Y of a cell membrane (using Equation 1) decreases from very high $Y = 10^7$ Pa (for $\sigma = 1/3$ indicating a behavior like a solid) down to $Y = 600$ Pa, if $\sigma = 0.49999$ describes a fluid-like behavior. The measured Y in Table 2 demonstrates that we may expect Y a few thousand Pa for normal cells and only a few hundred Pa for the corresponding tumor cells [139–142]. Generally, the stiffness decreases with increasing aggressiveness and invasiveness of tumor cells.

In summary, the membrane stiffness Y of aggressive tumor cells ranges from 200 to 800 Pa, leading to resonant frequencies between 10 Hz and 10 kHz (see above), while normal cells do not resonate or have less resonance in this frequency window. Furthermore, because of the typical microenvironment, tumor cells are isolated and surrounded by extracellular fluid.

Table 2. Literature data of Young's modulus for various cell lines comparing normal tissue cells and associated tumor cells arranged according to invasiveness top down.

Cell type	Reference	Y [Pa]
Theoretical cell:	Boal [135]	
$\sigma = 1/3$ (solid)		10,000,000
$\sigma = 0.49$		600,000
$\sigma = 0.499$		60,000
$\sigma = 0.4999$		6000
$\sigma = 0.49999$ (near fluid)		600
Lung:	Cross et al. [139]	
"normal"		2100
NSCLC		540
Breast:	Cross et al. [139]	
"normal"		1930
Adenocarcinoma		500
Breast:	Jonas et al. [140]	
MCF-10A (benign)		478
MDA-MB-231 (invasive)		341
Colon:	Jonas et al. [140]	
SW480 (non-invasive)		466
Hacat (invasive)		384
Lung:	Jonas et al. [140]	
A431 (non-invasive)		374
A125 (invasive)		265
Breast:	Smolyakov et al. [141]	
SKBR3/MCF7		630
BT474		410
MDA-MB231		270
Ovary:	Xu et al. [142]	
IOSE (non-malignant)		2472
OVCR4		1120
HEY		884
OVCaR3		576
HEYA8		494

For the theoretical estimations, we used $K_V \sim 10^7$ Pa of red cells [135] and the relationship for the Young's modulus Y [Pa] $= 3 \times (1 - 2\sigma) \times K_V$. The Poisson's ratio σ for red cells is $>1/3$ and indicates decreasing stiffness (increasing bending elasticity) if σ approaches $1/2$. Note $\sigma = 1/3$ for solids and $\sigma = 1/2$ for fluids.

Such single cells are more susceptible to an incident AM-RF and show the theoretically predicted resonance behavior. In comparison, normal cells are connected to one another in a tissue and show a different—presumably significantly lower resonance behavior—at higher frequencies. The different mechanical properties of tumor cells and tissues can increase the therapeutic ratio of AM-RF if an appropriate modulation frequency spectrum is selected; data suggest that lower frequencies <1 kHz are more effective.

We hypothesize that a large number of ion channels demodulate the AM-RF and transfer these low-frequency oscillations (in time to the AM frequency) mechanically to the membrane. Then, parts of the cell membranes or the entire cells oscillate in resonance with considerable displacements. In extreme cases of mechanical stress, the membrane might rupture, creating a hole. Such a long-dated water channel between the extracellular and intracellular space will cause ion fluxes along the concentration gradient that predominantly increases the Ca^{2+} load in the cell, but might also lead to other ion imbalances (Na^+, Cl^-, K^+ and pH). Less pronounced membrane vibrations at lower SAR levels might cause depolarization of the membrane potential or directly open ion channels by distortion of the voltage sensor or gate. Likely, T-type VGCCs that have already been identified open at low depolarization (of only $10 - 20$ mV) with consequential calcium influx into the cell (see Table 1).

Due to these oscillations, we expect a variety of membrane changes, especially on ion channels, when we examine different levels of SAR and different frequencies. Further systematic investigations with different parameters of AM-RF-HT are therefore worthwhile. In particular, we expect a strong interdependence of membrane properties on temperature and future experiments should examine these interactions. Relevant changes in the membrane properties, e.g., decreasing stiffness Y, are expected even at low temperature increases to 38 or 39 °C.

6. Discussion and prospects for oncologic applications

Clinical and preclinical data suggest the existence of antiproliferative non-thermal effects (Sections 3 and 4), which can damage tumor cells at lower temperatures (<42 °C) with low (1–2 W/kg) to moderate (5–25 W/kg) or high (300 W/kg) SAR levels. Because of $E \sim \mathrm{SAR}^{1/2}$ spreading of E is not as high ranging from $E \approx 50$ V/m (at 1 W/kg) to $E \approx 200$ V/m (at 25 W/kg) and up to $E \approx 800$ V/m (at 300 W/kg). Because the investigated non-thermal effects are caused predominantly by the E-field, measurable effects are already expectable at a low SAR of 1 W/kg under certain conditions.

A plethora of publications examined possible genotoxic effects of mobile phones [143–147] applying the mobile-specific frequencies around 900 MHz, 1800 MHz or 1950 MHz. The investigators found several biological effects, in particular, DNA damages that they attributed to the functionality of DNA as a fractal, i.e. broadband, antenna [148]. Yakymenko et al. [149,150] identified oxygen species overproduction reactive to mobile-specific EMF as a major correlate, and described several possible mechanisms in their reviews. Panagopoulos et al. [151] elaborated the concept that free ions on both sides of the cell membrane can oscillate and might cause membrane disorders. Interestingly, most of these studies confirmed our educated guesses that modulated and/or pulsed fields are more effective than non-modulated sinusoidal MW, e.g., [143,144,146]. These researchers confined themselves to the risks of mobile phones and did not discuss possible therapeutic applications. Some of their results concerning modulation/pulsation are nevertheless of interest for therapeutic applications. Note that these frequencies have only minor applicability for therapeutic purposes because of their limited penetration depth.

Our overview is intended to show that non-thermal effects exist in the RF range of $10 - 30$ MHz that can be exploited for therapeutic purposes as a further development of conventional hyperthermia. Microscopic hot spots, which are often cited as an explanation for alleged non-thermal effects, were discussed in detail and could largely be excluded both in the clinical studies discussed and in the preclinical experiments (Section 5.1). Instead, we presented possible mechanisms at ion channels for non-thermal effects of sinusoidal RF (Section 5.2). The data suggest that additional AM with selected (tumor-specific) modulation frequencies might enhance the antiproliferative effects of sinusoidal RF (Sections 3.3 and 4.3). We presented membrane resonances as a possible explanation for such frequency-dependent behavior and could correlate the observed modulation frequencies (hertz to kilohertz) with elastic membrane properties that are characteristic for tumor cells (Section 5.3).

These novel model approaches give some insight into possible mechanisms of non-thermal effects, but do not claim to be validated models that can quantitatively describe the experiments. The exact mechanisms and the dependencies of non-thermal effects are still unresolved and require much more data that cover broader ranges of SAR, temperatures and modulation frequency spectra as treatment parameters. Until now, the data regarding non-thermal effects for therapeutic purposes are not nearly comparable to the scope of the data on WB-HT and cRF-HT.

In particular, there is a lack of comparative measurements of RF ± AM in cells and experimental tumors in order to quantitatively record the influence of AM and enable refinement of the theoretical approaches. Interestingly, in the preclinical investigations with the mEHT, the data on the AM were incompletely documented and apparently, no systematic variation was performed (Section 4.1). Such comparative experiments are urgently needed.

However, the available data together indicate that the feasibility, tolerance and effectiveness of optimized AM-RF-HT might be distinctly superior to cRF-HT. AM-RF at 27.12 MHz (TheraBionic) refers to some frequency-dependent non-thermal effects at very low SAR (<0.4–2 W/kg) but is of limited clinical effectiveness and requires long exposition times.

The AM-RF-HT at 13.56 MHz promises higher effectiveness with a few sessions of one hour per week [23]. The existing data on AM-RF-HT suggest that low AM frequencies less than kilohertz might be more effective. At these low frequencies, the resonance of whole cells might be explained by forced oscillations of a variety of ion channels.

In preclinical studies, application of AM-RF-HT at 13.56 MHz (mEHT) alone at moderate clinically feasible SAR levels (<20–30 W/kg) and temperatures (<41–42 °C) might achieve an estimated cell kill of 30–50% in the target region, which is not achieved by RF-HT at temperatures ≤42 °C (see [69]). Therefore, AM-RF-HT monotherapy at 13.56 MHz is a debatable option. For example, if we integrate 2–3 AM-RF-HT at 13.56 MHz sessions per week up to a total of 20 sessions into an adjuvant scheme, this procedure might be comparable to 20×2 Gy with respect to cytotoxicity, taking into account preclinical data. Preclinical results confirmed *in vivo* that a series of AM-RF-HT monotherapy sessions with 48 h intervals (2–3 times a week) might be effective [63]. This is a clear deviation from the rules of cRF-HT, which requires a combination of RT and/or chemotherapy.

Available RF heating technology is suitable for exposing anatomical regions such as the brain, liver, lung, and major parts of the abdomen or pelvis. However, we require high SAR [W/kg] for temperatures >42 °C [temperature increase (ΔT) = 4.5 °C from 37.5 °C to 42 °C] in a target with perfusion w [ml/100 g/min] as given by the following easy relationship [152]:

$$\mathrm{SAR}\ [\mathrm{W/kg}] = (\Delta T/1.4) \times w\ [\mathrm{ml/100\ g/min}]$$

Only for $w < 10$ ml/100 g/min are SAR of ≈30 W/kg sufficient, which are achievable using the elaborated APA technique. The less expensive capacitive technology might achieve 10–15 W/kg in deep anatomical regions. Therefore, only in low-perfused tumors or tissues with $w < 5$ ml/100 g/min capacitive systems can gain temperatures >42 °C.

Considering the non-thermal effects outlined in this review, we expect relevant cytotoxicity at moderate SAR and lower temperatures <42 °C significantly reducing the high demands for cRF-HT listed in quality assurance reports [10]. There is evidence that a pure RF has non-thermal antiproliferative effects [55], whereby an RF of 10 MHz might have advantages over 100 MHz (see Section 5.1). Further, preclinical and clinical studies strongly suggest that a suitable AM can increase RF effectiveness. However, we do not know exactly the optimal modulation frequencies, SAR, and temperatures for clinical applications. Therefore, further systematic preclinical studies are required to complete the fragmentary data on non-thermal effects.

For cRF-HT, only tumors with low perfusion <10 ml/100 g/min are accessible for SAR = 30 W/kg to achieve 42–43 °C; even tumors with perfusion up to 40 ml/100 g/min would be accessible for the same SAR if temperatures of 38 °C would be considered sufficient to ensure non-thermal antiproliferative effects in conjunction with a slight temperature increase (see the equation above). Here, we regard temperature as a co-variable. Consequently, the possible applications in oncology would increase considerably. These applications include AM-RF-HT monotherapy but especially in combination with other therapy modalities. If the existence of non-thermal antiproliferative effects can be further substantiated, we believe a new field opens up for oncology.

Author contributions

P.W. conceptualization of the project, review of the literature, development of the theory and performance of calculations, writing and approval of the manuscript. U.S. editing and approval of the manuscript. P.G. funding acquisition, the conceptualization of the project, methodology, writing and approval of the manuscript. All authors have read and agreed to the published version of the manuscript.

Disclosure statement

No potential conflict of interest was reported by the author(s).

Funding

We acknowledge support from the Berliner Krebsgesellschaft e.V., grant number GHFF202006, www.berliner-krebsgesellschaft.de, and from the German Research Foundation (DFG) and the Open Access Publication Fund of Charité – Universitätsmedizin Berlin.

References

[1] Wust P, Hildebrandt B, Sreenivasa G, et al. Hyperthermia in combined treatment of cancer. Lancet Oncol. 2002;3(8):487–497.
[2] Issels RD, Lindner LH, Verweij J, et al. Effect of neoadjuvant chemotherapy plus regional hyperthermia on long-term outcomes among patients with localized high-risk soft tissue sarcoma: the EORTC 62961-ESHO 95 randomized clinical trial. JAMA Oncol. 2018;4(4):483–492.
[3] Van Der Zee J, Gonzalez Gonzalez D, Van Rhoon GC, et al. Comparison of radiotherapy alone with radiotherapy plus hyperthermia in locally advanced pelvic tumours: a prospective, randomised, multicentre trial. Lancet. 2000;355(9210):1119–1125.
[4] Harima Y, Nagata K, Harinma K, et al. A randomized clinical trial of radiation therapy versus thermoradiotherapy in stage III cervical carcinoma. Int J Hyperthermia. 2001;17:97–105.
[5] Harima Y, Ohguri T, Imada H, et al. A multicentre randomised clinical trial of chemoradiotherapy plus hyperthermia versus chemoradiotherapy alone in patients with locally advanced cervical cancer. Int J Hyperthermia. 2016;32(7):801–808.
[6] Vernon CC, Hand JW, Field SB, et al. Radiotherapy with or without hyperthermia in the treatment of superficial localized breast cancer: results from five randomized controlled trials. International collaborative hyperthermia group. Int J Radiat Oncol Biol Phys. 1996;35(4):731–744.
[7] Jones EL, Oleson JR, Prosnitz LR, et al. Randomized trial of hyperthermia and radiation for superficial tumors. J Clin Oncol. 2005;23(13):3079–3085.
[8] Van Der Zee J, De Bruijne M, Mens JWM, et al. Reirradiation combined with hyperthermia in breast cancer recurrences: overview of experience in Erasmus MC. Int J Hyperthermia. 2010;26(7):638–648.
[9] Overgaard J, Gonzalez Gonzalez D, Hulshof MC, et al. Randomised trial of hyperthermia as adjuvant to radiotherapy for recurrent or metastatic malignant melanoma. Lancet. 1995;345(8949):540–543.
[10] Lagendijk JJ, Van Rhoon GC, Hornsleth SN, et al. ESHO quality assurance guidelines for regional hyperthermia. Int J Hyperthermia. 1998;14(2):125–133.
[11] Kok HP, Cressman EN, Ceelen W, et al. Heating technology for malignant tumors: a review. Int J Hyperthermia. 2020;37(1):711–741.
[12] Dewey WC, Hopwood LE, Sapareto SA, et al. Cellular responses to combinations of hyperthermia and radiation. Radiology. 1977;123(2):463–474.
[13] Hahn GM. Potential for therapy of drugs and hyperthermia. Cancer Res. 1979;39(6 Pt 2):2264–2268.
[14] Overgaard J. Simultaneous and sequential hyperthermia and radiation treatment of an experimental tumor and its surrounding normal tissue in vivo. Int J Radiat Oncol Biol Phys. 1980;6(11):1507–1517.
[15] Urano M, Kahn J, Majima H, et al. The cytotoxic effect of cis-diamminedichloroplatinum(II) on cultured Chinese hamster ovary cells at elevated temperatures: Arrhenius plot analysis . Int J Hyperthermia. 1990;6(3):581–590.
[16] Franken NAP, Oei AL, Kok HP, et al. Cell survival and radiosensitisation: modulation of the linear and quadratic parameters of the LQmodel (review). Int J Oncol. 2013;42(5):1501–1515.
[17] Mei X, Ten Cate R, Van Leeuwen CM, et al. Radiosensitization by hyperthermia: the effects of temperature, sequence, and time Interval in cervical cell lines. Cancers. 2020;12(3):582.
[18] Franckena M, Fatehi D, de Bruijne M, et al. Hyperthermia dose-effect relationship in 420 patients with cervical cancer treated with combined radiotherapy and hyperthermia. Eur J Cancer. 2009;45(11):1969–1978.
[19] Dinges S, Harder C, Wurm R, et al. Combined treatment of inoperable carcinomas of the uterine cervix with radiotherapy and regional hyperthermia. Results of a phase II trial. Strahlenther Onkol. 1998;174(10):517–521.

[20] Sreenivasa G, Hildebrandt B, Kümmel S, et al. Radiochemotherapy combined with regional pelvic hyperthermia induces high response and resectability rates in patients with nonresectable cervical cancer >/=FIGO IIB "bulky". Int J Radiat Oncol Biol Phys. 2006;66(4):1159–1167.
[21] Tilly W, Wust P, Rau B, et al. Temperature data and specific absorption rates in pelvic tumours: predictive factors and correlations. Int J Hyperthermia. 2001;17(2):172–188.
[22] Hildebrandt B, Hegewisch-Becker S, Kerner T, et al. Current status of radiant whole-body hyperthermia at temperatures >41.5 degrees C and practical guidelines for the treatment of adults. The German 'interdisciplinary working group on hyperthermia'. Int J Hyperthermia. 2005;21(2):169–183.
[23] Minnaar CA, Kotzen JA, Ayeni OA, et al. The effect of modulated electro-hyperthermia on local disease control in HIV-positive and -negative cervical cancer women in South Africa: early results from a phase III randomised controlled trial. PLOS One. 2019;14(6):e0217894.
[24] Minnaar CA, Kotzen JA, Naidoo T, et al. Analysis of the effects of mEHT on the treatment-related toxicity and quality of life of HIV-positive cervical cancer patients. Int J Hyperthermia. 2020; 37(1):263–272.
[25] Stupp R, Taillibert S, Kanner A, et al. Effect of tumor-treating fields plus maintenance temozolomide vs. maintenance temozolomide alone on survival in patients with glioblastoma: a randomized clinical trial. JAMA. 2017;318(23):2306–2316.
[26] Barbault A, Costa FP, Bottger B, et al. Amplitude-modulated electromagnetic fields for the treatment of cancer: discovery of tumor-specific frequencies and assessment of a novel therapeutic approach. J Exp Clin Cancer Res. 2009;28(1):51.
[27] Costa FP, De Oliveira AC, Meirelles R, et al. Treatment of advanced hepatocellular carcinoma with very low levels of amplitude-modulated electromagnetic fields. Br J Cancer. 2011; 105(5):640–648.
[28] Szasz AM, Minnaar CA, Szentmártoni G, et al. Review of the clinical evidences of modulated electro-hyperthermia (mEHT) method: an update for the practicing oncologist. Front Oncol. 2019;9:1012.
[29] Lee SY, Lee NR, Cho DH, et al. Treatment outcome analysis of chemotherapy combined with modulated electro-hyperthermia compared with chemotherapy alone for recurrent cervical cancer, following irradiation. Oncol Lett. 2017;14(1):73–78.
[30] Lee SY, Kim JH, Han YH, et al. The effect of modulated electrohyperthermia on temperature and blood flow in human cervical carcinoma. Int J Hyperthermia. 2018;34(7):953–960.
[31] Fiorentini G, Sarti D, Milandri C, et al. Modulated electrohyperthermia in integrative cancer treatment for relapsed malignant glioblastoma and astrocytoma: retrospective multicenter controlled study. Integr Cancer Ther. 2019;18:1534735418812691.
[32] Stupp R, Hegi ME, Mason WP, et al. Effects of radiotherapy with concomitant and adjuvant temozolomide versus radiotherapy alone on survival in glioblastoma in a randomised phase III study: 5-year analysis of the EORTC-NCIC trial. Lancet Oncol. 2009;10(5):459–466.
[33] Hager ED, Dziambor H, Hohmann D, et al. Deep hyperthermia with radiofrequencies in patients with liver metastases from colorectal cancer. Anticancer Res. 1999;19(4):3403–3408.
[34] Lok E, San P, Hua V, et al. Analysis of physical characteristics of tumor treating fields for human glioblastoma. Cancer Med. 2017;6(6):1286–1300.
[35] Miranda PC, Mekonnen A, Salvador R, et al. Predicting the electric field distribution in the brain for the treatment of glioblastoma. Phys Med Biol. 2014;59(15):4137–4147.
[36] Wenger C, Salvador R, Basser PJ, et al. The electric field distribution in the brain during TTFields therapy and its dependence on tissue dielectric properties and anatomy: a computational study. Phys Med Biol. 2015;60(18):7339–7357.
[37] Ballo MT, Urman N, Lavy-Shahaf G, et al. Correlation of tumor treating fields dosimetry to survival outcomes in newly diagnosed glioblastoma: a large-scale numerical simulation-based analysis of data from the phase 3 EF-14 randomized trial. Int J Radiat Oncol Biol Phys. 2019;104(5):1106–1113.
[38] Bakitas MA, Tosteson TD, Li Z, et al. Early versus delayed initiation of concurrent palliative oncology care: patient outcomes in the ENABLE III randomized controlled trial. J Clin Oncol. 2015; 33(13):1438–1445.
[39] Mun EJ, Babiker HM, Weinberg U, et al. Tumor-treating fields: a fourth modality in cancer treatment. Clin Cancer Res. 2018;24(2): 266–275.
[40] Sharma S, Wu SY, Jimenez H, et al. Ca^{2+} and CACNA1H mediate targeted suppression of breast cancer brain metastasis by AM RF EMF. EBioMedicine. 2019;44:194–208.
[41] Feychting M, Ahlbom A, Kheifets L. EMF and health. Annu Rev Public Health. 2005;26:165–189.
[42] Kheifets L, Bowman JD, Checkoway H, et al. Future needs of occupational epidemiology of extremely low frequency electric and magnetic fields: review and recommendations. Occup Environ Med. 2009;66(2):72–80.
[43] Foster KR. Thermal and nonthermal mechanisms of interaction of radio-frequency energy with biological systems. IEEE Trans Plasma Sci. 2000;28(1):15–23.
[44] Adair RK. Biophysical limits on athermal effects of RF and microwave radiation. Bioelectromagnetics. 2003;24(1):39–48.
[45] Ahlbom A, Green A, Kheifets L, et al. Epidemiology of health effects of radiofrequency exposure. Environ Health Perspect. 2004;112(17):1741–1754.
[46] Litvak E, Foster KR, Repacholi MH. Health and safety implications of exposure to electromagnetic fields in the frequency range 300 Hz to 10 MHz. Bioelectromagnetics. 2002;23(1):68–82.
[47] Schuderer J, Oesch W, Felber N, et al. In vitro exposure apparatus for ELF magnetic fields. Bioelectromagnetics. 2004;25(8):582–591.
[48] Schuderer J, Spat D, Samaras T, et al. In vitro exposure systems for RF exposures at 900 MHz. IEEE Trans Microwave Theory Techn. 2004;52(8):2067–2075.
[49] Schuderer J, Samaras T, Oesch W, et al. High peak SAR exposure unit with tight exposure and environmental control for in vitro experiments at 1800 MHz. IEEE Trans Microwave Theory Techn. 2004;52(8):2057–2066.
[50] Kuster N, Schönborn F. Recommended minimal requirements and development guidelines for exposure setups of bio-experiments addressing the health risk concern of wireless communications. Bioelectromagnetics. 2000;21(7):508–514.
[51] Greenebaum B, Barnes F. Handbook of biological effects of electromagnetic fields. 4th ed. Vol. 1, Biological and medical aspects of electromagnetic fields. Boca Raton: CRC Press;2019.
[52] Greenebaum B, Barnes F. Handbook of biological effects of electromagnetic fields. 4th ed. Vol. 2, Bioengineering and biophysical aspects of electromagnetic fields. Boca Raton: CRC Press; 2019.
[53] Verrender A, Loughran SP, Dalecki A, et al. Pulse modulated radiofrequency exposure influences cognitive performance. Int J Radiat Biol. 2016;92(10):603–610.
[54] Miyakoshi J. Cellular and molecular responses to radio-frequency electromagnetic fields. Proc IEEE. 2013;101(6):1494–1502.
[55] Wust P, Kortüm B, Strauss U, et al. Non-thermal effects of radiofrequency electromagnetic fields. Scientific Rep. 2020;10:13488.
[56] Reitz JR, Milford FJ, Christy RW. Foundations of electromagnetic theory. 4th ed. Boston (MA): Addison-Wesley Publishing Company;2008.
[57] Szasz A, Szasz O, Iluri N, inventor. Radiofrequency hyperthermia device with targeted feedback signal modulation. United States Patent US 9,320,911 B2. 2016.
[58] Wust P, Ghadjar P, Nadobny J, et al. Physical analysis of temperature-dependent effects of amplitude-modulated electromagnetic hyperthermia. Int J Hyperthermia. 2019;36(1): 1245–1253.
[59] Schaefer H, Schwan H. On the question of selective heating small particles in the ultra-short wave capacitor field (Zur Frage der selektiven Erhitzung kleiner Teilchen im Ultrakurzwellen-Kondensatorfeld). Ann Phys. 1943;435(1–2):99–135.

[60] Rabin Y. Is intracellular hyperthermia superior to extracellular hyperthermia in the thermal sense? Int J Hyperthermia. 2002; 18(3):194–202.
[61] Yamada K, Oda T, Hashimoto S, et al. Minimally required heat doses for various tumour sizes in induction heating cancer therapy determined by computer simulation using experimental data. Int J Hyperthermia. 2010;26(5):465–474.
[62] Hedayati M, Thomas O, Abubaker-Sharif B, et al. The effect of cell cluster size on intracellular nanoparticle-mediated hyperthermia: is it possible to treat microscopic tumors? Nanomedicine). 2013;8(1):29–41.
[63] Danics L, Schvarcz CA, Viana P, et al. Exhaustion of protective heat shock response 2 induces significant tumor damage by apoptosis 3 after modulated electro-hyperthermia treatment of 4 triple negative breast cancer isografts in mice. Cancers. 2020;12(9):2581.
[64] Krenacs T, Meggyeshazi N, Forika G, et al. Modulated electro-hyperthermia-induced tumor damage mechanisms revealed in cancer models. IJMS. 2020;21(17):6270.
[65] Andocs G, Renner H, Balogh L, et al. Strong synergy of heat and modulated electromagnetic field in tumor cell killing. Strahlenther Onkol. 2009;185(2):120–126.
[66] Tsang YW, Huang CC, Yang KL, et al. Improving immunological tumor microenvironment using electro-hyperthermia followed by dendritic cell immunotherapy. BMC Cancer. 2015;15:708.
[67] Yang KL, Huang CC, Chi MS, et al. In vitro comparison of conventional hyperthermia and modulated electro-hyperthermia. Oncotarget. 2016;7(51):84082–84092.
[68] Andocs G, Rehman MU, Zhao QL, et al. Comparison of biological effects of modulated electro-hyperthermia and conventional heat treatment in human lymphoma U937 cells. Cell Death Discov. 2016;2:16039.
[69] Andocs G, Rehman MU, Zhao QL, et al. Nanoheating without artificial nanoparticles part II. Experimental support of the nanoheating concept of the modulated electro-hyperthermia method, using U937 cell suspension model. Biol Med. 2015;07(04):1.
[70] Meggyesházi N, Andócs G, Spisák S, et al. Early changes in mRNA and protein expression related to cancer treatment by modulated electrohyperthermia Conference Papers in Medicine; 2012 Oct 12–14; Budapest, Hungary; Vol. 2013; Hindawi.
[71] Meggyesházi N, Andocs G, Balogh L, et al. DNA fragmentation and caspase-independent programmed cell death by modulated electrohyperthermia. Strahlenther Onkol. 2014;190(9):815–822.
[72] Andocs G, Meggyeshazi N, Balogh L, et al. Upregulation of heat shock proteins and the promotion of damage-associated molecular pattern signals in a colorectal cancer model by modulated electrohyperthermia. Cell Stress Chaperones. 2015;20(1):37–46.
[73] Cha J, Jeon TW, Lee CG, et al. Electro-hyperthermia inhibits glioma tumorigenicity through the induction of E2F1-mediated apoptosis. Int J Hyperthermia. 2015;31(7):784–792.
[74] Jeon TW, Yang H, Lee CG, et al. Electro-hyperthermia up-regulates tumour suppressor Septin 4 to induce apoptotic cell death in hepatocellular carcinoma. Int J Hyperthermia. 2016;32(6):648–656.
[75] Vancsik T, Kovago C, Kiss E, et al. Modulated electro-hyperthermia induced loco-regional and systemic tumor destruction in colorectal cancer allografts. J Cancer. 2018;9(1):41–53.
[76] Vancsik T, Forika G, Balogh A, et al. Modulated electro-hyperthermia induced p53 driven apoptosis and cell cycle arrest additively support doxorubicin chemotherapy of colorectal cancer in vitro . Cancer Med. 2019i8(9):4292–4303.
[77] Besztercei B, Vancsik T, Benedek A, et al. Stress-induced, p53-mediated tumor growth inhibition of melanoma by modulated electrohyperthermia in mouse models without major immunogenic effects. IJMS. 2019;20(16):4019.
[78] Garg AD, Martin S, Golab J, et al. Danger signalling during cancer cell death: origins, plasticity and regulation. Cell Death Differ. 2014;21(1):26–38.
[79] Hernandez C, Huebener P, Schwabe RF. Damage-associated molecular patterns in cancer: a double-edged sword. Oncogene. 2016;35(46):5931–5941.
[80] Qin W, Akutsu Y, Andocs G, et al. Modulated electro-hyperthermia enhances dendritic cell therapy through an abscopal effect in mice. Oncol Rep. 2014;32(6):2373–2379.
[81] Kim W, Kim MS, Kim HJ, et al. Role of HIF-1α in response of tumors to a combination of hyperthermia and radiation in vivo. Int J Hyperthermia. 2018;34(3):276–283.
[82] McDonald M, Corde S, Lerch M, et al. First in vitro evidence of modulated electro-hyperthermia treatment performance in combination with megavoltage radiation by clonogenic assay. Sci Rep. 2018;8(1):1–3.
[83] Prasad B, Kim S, Cho W, et al. Quantitative estimation of the equivalent radiation dose escalation using radiofrequency hyperthermia in mouse xenograft models of human lung cancer. Sci Rep. 2019;9(1):3942.
[84] Forika G, Balogh A, Vancsik T, et al. Modulated electro-hyperthermia resolves radioresistance of Panc1 pancreas adenocarcinoma and promotes DNA damage and apoptosis in vitro. IJMS. 2020;21(14):5100.
[85] Tsang YW, Chi KH, Huang CC, et al. Modulated electro-hyperthermia-enhanced liposomal drug uptake by cancer cells. Int J Nanomedicine. 2019;14:1269–1279.
[86] Kirson ED, Gurvich Z, Schneiderman R, et al. Disruption of cancer cell replication by alternating electric fields. Cancer Res. 2004;64(9):3288–3295.
[87] Kirson ED, Dbalý V, Tovaryš F, et al. Alternating electric fields arrest cell proliferation in animal tumor models and human brain tumors. Proc Natl Acad Sci USA. 2007;104(24):10152–10157.
[88] Kirson ED, Schneiderman RS, Dbalý V, et al. Chemotherapeutic treatment efficacy and sensitivity are increased by adjuvant alternating electric fields (TTFields). BMC Med Phys. 2009;9(1):1–3.
[89] Silginer M, Weller M, Stupp R, et al. Biological activity of tumor-treating fields in preclinical glioma models. Cell Death Dis. 2017; 8(4):e2753.
[90] Zimmerman JW, Jimenez H, Pennison MJ, et al. Targeted treatment of cancer with radiofrequency electromagnetic fields amplitude-modulated at tumor-specific frequencies. Chin J Cancer. 2013;32(11):573–581.
[91] Zimmerman JW, Pennison MJ, Brezovich I, et al. Cancer cell proliferation is inhibited by specific modulation frequencies. Br J Cancer. 2012;106(2):307–313.
[92] Jimenez H, Wang M, Zimmerman JW, et al. Tumour-specific amplitude-modulated radiofrequency electromagnetic fields induce differentiation of hepatocellular carcinoma via targeting $Ca_v3.2$ T-type voltage-gated calcium channels and Ca^{2+} influx . EBioMedicine. 2019;44:209–224.
[93] Taylor JT, Zeng XB, Pottle JE, et al. Calcium signaling and T-type calcium channels in cancer cell cycling. World J Gastroenterol. 2008;14(32):4984–4991.
[94] Buckner CA, Buckner AL, Koren SA, et al. Inhibition of cancer cell growth by exposure to a specific time-varying electromagnetic field involves T-type calcium channels. PLOS One. 2015; 10(4):e0124136.
[95] Phan NN, Wang CY, Chen CF, et al. Voltage-gated calcium channels: novel targets for cancer therapy. Oncol Lett. 2017;14(2): 2059–2074.
[96] Pickard WF, Moros EG. Energy deposition processes in biological tissue: nonthermal biohazards seem unlikely in the ultra-high frequency range. Bioelectromagnetics. 2001;22(2):97–105.
[97] Adair RK. Vibrational resonances in biological systems at microwave frequencies. Biophys J. 2002;82(3):1147–1152.
[98] Adair RK. Noise and stochastic resonance in voltage-gated ion channels. Proc Natl Acad Sci USA. 2003;100(21):12099–12104.
[99] Foster KR, Repacholi MH. Biological effects of radiofrequency fields: does modulation matter? Radiat Res. 2004;162(2):219–225.

[100] Prohofsky EW. RF absorption involving biological macromolecules. Bioelectromagnetics. 2004;25(6):441–451.
[101] Fröhlich H. Long-range coherence and energy storage in biological systems. Int J Quantum Chem. 1968;2(5):641–649.
[102] Edwards GS, Davis CC, Saffer JD, et al. Resonant microwave absorption of selected DNA molecules. Phys Rev Lett. 1984; 53(13):1284–1287.
[103] Foster KR, Baish JW. Viscous damping of vibrations in microtubules. J Biol Phys. 2000;26(4):255–260.
[104] Wust P, Gneveckow U, Johannsen M, et al. Magnetic nanoparticles for interstitial thermotherapy-feasibility, tolerance and achieved temperatures. Int J Hyperthermia. 2006;22(8):673–685.
[105] Wust P. Thermotherapy in oncology. Bremen: UNI-MED Verlag AG; 2016.
[106] Dutz S, Hergt R. Magnetic nanoparticle heating and heat transfer on a microscale: basic principles, realities and physical limitations of hyperthermia for tumour therapy. Int J Hyperthermia. 2013;29(8):790–800.
[107] Foster KR, Schwan HP. Dielectric properties of tissues and biological materials: a critical review. Crit Rev Biomed Eng. 1989; 17(1):25–104.
[108] Eibert TF, Alaydrus M, Wilczewski F, et al. Electromagnetic and thermal analysis for lipid bilayer membranes exposed to RF fields. IEEE Trans Biomed Eng. 1999;46(8):1013–1020.
[109] Martinsen OG, Grimnes S, Schwan HP. Interface phenomena and dielectric properties of biological tissue. Encyclopedia of Surface and Colloid Science. 2002;20:2643–2653.
[110] Stoy RD, Foster KR, Schwan HP. Dielectric properties of mammalian tissues from 0.1 to 100 MHz: a summary of recent data. Phys Med Biol. 1982;27(4):501–513.
[111] Papp E, Vancsik T, Kiss E, et al. Energy absorption by the membrane rafts in the modulated electro-hyperthermia (mEHT). OJBIPHY. 2017;07(04):216–229.
[112] Doyle DA, Cabral JM, Pfuetzner RA, et al. The structure of the potassium channel: molecular basis of K + conduction and selectivity. Science. 1998;280(5360):69–77.
[113] Hille B. Ion channels of excitable membranes. 3rd ed. Sunderland: Sinauer Associates Inc.;2001.
[114] Friedman MH. Principles and models of biological transport. 2nd ed. New York: Springer Science + Media;2010.
[115] Berg JM, Tymoczko J, Gatto GJ, et al. Biochemistry. 9th ed. New York: W.H. Freeman;2019.
[116] Neuhaus E, Zirjacks L, Ganser K, et al. Alternating electric fields (TTFields) activate Cav1.2 channels in human glioblastoma cells. Cancers. 2019;11(1):110.
[117] Pall ML. Electromagnetic fields act *via* activation of voltage-gated calcium channels to produce beneficial or adverse effects . J Cell Mol Med. 2013;17(8):958–965.
[118] Yamakage M, Namiki A. Calcium channels-basic aspects of their structure, function and gene encoding; anesthetic action on the channels-a review. Can J Anaesth. 2002;49(2):151–164.
[119] Huber SM. Oncochannels. Cell Calcium. 2013;53(4):241–255.
[120] Fraser SP, Pardo LA. Ion channels: functional expression and therapeutic potential in cancer. Colloquium on ion channels and cancer. EMBO Rep. 2008;9(6):512–515.
[121] Stühmer W, Pardo LA. K(+) channels as therapeutic targets in oncology. Future Med Chem. 2010;2(5):745–755.
[122] Becchetti A. Ion channels and transporters in cancer. 1. Ion channels and cell proliferation in cancer. Am J Physiol Cell Physiol. 2011;301(2):C255–65.
[123] Santoni G, Farfariello V. TRP channels and cancer: new targets for diagnosis and chemotherapy. Endocr Metab Immune Disord Drug Targets. 2011;11(1):54–67.
[124] Pardo LA, Stühmer W. The roles of K(+) channels in cancer. Nat Rev Cancer. 2014;14(1):39–48.
[125] Lang F, Stournaras C. Ion channels in cancer: future perspectives and clinical potential. Philos Trans R Soc Lond B Biol Sci. 2014; 369(1638):20130108.
[126] Santoni G, Maggi F, Morelli MB, et al. Transient receptor potential cation channels in cancer therapy. Medical Sciences. 2019; 7(12):108.
[127] Ashrafuzzaman M. Nanoscale biophysics of the cell. New York: Springer International Publishing AG;2018.
[128] Bawin SM, Kaczmarek LK, Adey WR. Effects of modulated VHF fields on the central nervous system. Ann N Y Acad Sci. 1975; 247(1):74–81.
[129] Blackman CF, Benane SG, Elder JA, et al. Induction of calcium-ion efflux from brain tissue by radiofrequency radiation: effect of sample number and modulation frequency on the power-density window . Bioelectromagnetics. 1980;1(1):35–43.
[130] Blackman CF, Benane SG, Kinney LS, et al. Effects of ELF fields on calcium-ion efflux from brain tissue in vitro. Rad Res. 1982; 92(3):510–520.
[131] Blackman CF, Benane SG, House DE. The influence of temperature during electric- and magnetic-field-induced alteration of calcium-ion release from in vitro brain tissue. Bioelectromagnetics. 1991;12(3):173–182.
[132] Merritt JH, Chamness AF, Shelton WW. Attempts to alter $45Ca^{2+}$ binding to brain tissue with pulse-modulated microwave energy. Bioelectromagnetics. 1982;3(4):475–478.
[133] Cranfield CG, Wood AW, Anderson V, et al. Effects of mobile phone type signals on calcium levels within human leukaemic T-cells (Jurkat cells). Int J Radiat Biol. 2001;77(12):1207–1217.
[134] Blackman CF. Treating cancer with amplitude-modulated electromagnetic fields: a potential paradigm shift, again? Br J Cancer. 2012;106(2):241–242.
[135] Boal D. Mechanics of the cell. 2nd ed. New York: Cambridge University Press;2012.
[136] Landau LD, Lifshitz EM. Theory of elasticity. Oxford: Pergamon Press;1986.
[137] Suresh S. Biomechanics and biophysics of cancer cells. Acta Biomater. 2007; 3(4):413–438.
[138] Katira P, Bonnecaze RT, Zaman MH. Modeling the mechanics of cancer: effect of changes in cellular and extra-cellular mechanical properties. Frontiers Oncol. 2013;3:145.
[139] Cross SE, Jin YS, Rao J, et al. Nanomechanical analysis of cells from cancer patients. Nat Nanotechnol. 2007;2(12):780–783.
[140] Jonas O, Mierke CT, Käs JA. Invasive cancer cell lines exhibit biomechanical properties that are distinct from their noninvasive counterparts. Soft Matter. 2011;7(24):11488–11495.
[141] Smolyakov G, Thiebot B, Campillo C, et al. Elasticity, adhesion, and tether extrusion on breast cancer cells provide a signature of their invasive potential. ACS Appl Mater Interfaces. 2016; 8(41):27426–27431.
[142] Xu W, Mezencev R, Kim B, et al. Cell stiffness is a biomarker of the metastatic potential of ovarian cancer cells. PLOS One. 2012; 7(10):e46609.
[143] Diem E, Schwarz C, Adlkofer F, et al. Non-thermal DNA breakage by mobile-phone radiation (1800 MHz) in human fibroblasts and in transformed GFSH-R17 rat granulosa cells in vitro. Mutat Res. 2005;583(2):178–183.
[144] Panagopoulos DJ, Chavdoula ED, Karabarbounis A, et al. Comparison of bioactivity between GSM 900 MHz and DCS 1800 MHz mobile telephony radiation. Electromagn Biol Med. 2007;26(1):33–44.
[145] Zhijian C, Xiaoxue L, Yezhen L, et al. Impact of 1.8-GHz radiofrequency radiation (RFR) on DNA damage and repair induced by doxorubicin in human B-cell lymphoblastoid cells. Mutat Res. 2010;695(1–2):16–21.
[146] Franzellitti S, Valbonesi P, Ciancaglini N, et al. Transient DNA damage induced by high-frequency electromagnetic fields (GSM 1.8 GHz) in the human trophoblast HTR-8/SVneo cell line evaluated with the alkaline comet assay. Mutat Res. 2010;683(1–2):35–42.

[147] Al-Serori H, Ferk F, Kundi M, et al. Mobile phone specific electromagnetic fields induce transient DNA damage and nucleotide excision repair in serum-deprived human glioblastoma cells. *PLOS One*. 2018;13(4):e0193677.

[148] Blank M, Goodman R. DNA is a fractal antenna in electromagnetic fields. Int J Radiat Biol. 2011;87(4):409–415.

[149] Yakymenko I, Sidorik E. Risks of carcinogenesis from electromagnetic radiation of mobile telephony devices. Exp Oncol. 2010; 32(2):54–60.

[150] Yakymenko I, Tsybulin O, Sidorik E, et al. Oxidative mechanisms of biological activity of low-intensity radiofrequency radiation. Electromagn Biol Med. 2016;35(2):186–202.

[151] Panagopoulos DJ, Messini N, Karabarbounis A, et al. A mechanism for action of oscillating electric fields on cells. Biochem Biophys Res Commun. 2000;272(3):634–640.

[152] Wust P, Cho CH, Hildebrandt B, et al. Thermal monitoring: invasive, minimal-invasive and non-invasive approaches. Int J Hyperthermia. 2006;22(3):255–262.